# Electronic Supporting Information

# Alkaline electrochemical water oxidation with multi-shelled cobalt manganese oxide hollow spheres

Arindam Indra, Prashanth W. Menezes, Chittaranjan Das, Dieter Schmiβer and Matthias Driess*

## Chemicals

All chemical reagents (analytical grade) were purchased from either Sigma Aldrich or Alfa Aesar and used as received without any further purification. Deionised water was used for the reactions and water oxidation experiments.

## Instruments

PXRD was recorded on a Bruker AXS D8 advanced automatic diffractometer equipped with a position sensitive detector (PSD) and a curved germanium (111*)* primary monochromator. The XRD profiles recorded were in the range of $5° < 2\theta < 80°$ by using Cu-*Kα* ($\lambda = 1.5418$ Å) radiation.

Carbon content was determined by the elemental analyses with Flash EA 112 Thermo Finnigan elemental analyzer. ICP-AES was measured on a Thermo Jarrell Ash Trace Scan analyzer. The samples were dissolved in aqua regia and the results of three independent measurements were averaged. BET surface area measurements of cobalt manganese oxides were carried out by using a 9-point $N_2$ adsorption analysis on a Micromeritics Gemini with VacPrep 061.

SEM-images were acquired with a Hitachi S-2700 microscope. TEM-investigations were performed by using FEI Tecnai $G^2$ 20 S-TWIN transmission electron microscope (FEI Company, Eindhoven, Netherlands) equipped with a $LaB_6$-source at 200kV acceleration voltage. EDX-analysis were carried out with an EDAX r-TEM SUTW Detector (Si (Li)-detector. Both SEM and TEM studies were carried out at the Zentrum für Elektronenmikroskopie (ZELMI) of Technische Universität Berlin.

The X-ray photoemission spectroscopy and X-ray absorption spectroscopy measurements were performed at BESSY-II, Berlin with beam line U49-PG/2. The X-ray beam was calibrated with nitrogen gas cell by using N 1s spectra and the analyzer was calibrated with Au 4f spectra. The measurements were carried out in ultra high vacuum environment. The XPS measurements were performed with Speclab analyzer while the NEXAF data were collected in the total electron yield (TEY) mode with a KYTHLE picoamperometer. The Co 2p, Mn 2p and O 1s photoemission spectra were measured with photon energy of 1100 eV.

In NEXAFS studies, the metal L edge was stimulated to excite electrons from 2p level to unoccupied 3d level. This technique can be used to determine the oxidation states of the elements with higher precision and can also probe into the chemical environment. Data analyses were performed by using Casa XPS (Casa Software Ltd.) and Vision data processing program (Kratos Analytical Ltd.).

## Experimental Section

### Synthesis of Carbon spheres

Carbon spheres are synthesized by the modified literature reported procedure. 2 g of glucose was dissolved in 30 mL water and heated at 170 °C in a Teflon coated autoclave for 6 h. The solid was centrifuged out, washed several times with water, finally with acetone and dried overnight in oven at 50 °C.[S1]

**Synthesis of $Co_2Mn$**

$Co(OAc)_2.4H_2O$ (1 g in 20 mL $H_2O$) and $Mn(OAc)_2.4H_2O$ (0.49 g in 20 mL $H_2O$) solutions were mixed together and added to previously prepared carbon spheres (400 mg). The whole mixture was stirred for 1 h, aged for 48 h and centrifuged out (8000 rpm) the solid and washed with ethanol (3 times) and dried at 50 °C in an air oven for 24 h. The dry powder was heated at 500 °C in synthetic air mixture for 1 h with a ramp of 2 °C $min^{-1}$ and cooled down naturally to room temperature. The solid powder was collected and designated as **$Co_2Mn$**.

Similarly, **CoMn** was synthesized by using $Co(OAc)_2.4H_2O$ (1 g in 20 ml $H_2O$) and $Mn(OAc)_2.4H_2O$ (0.98 g in 20 ml $H_2O$). **$CoMn_2$** was synthesized from $Co(OAc)_2.4H_2O$ (0.5 g in 20 ml $H_2O$) and $Mn(OAc)_2.4H_2O$ (0.98 g in 20 ml $H_2O$).

**Synthesis of B-$Co_2Mn$**

200 mg $Co(OAc)_2.4H_2O$ and 100 mg $Mn(OAc)_2.4H_2O$ were dissolved in minimum volume of water and stirred for 10 min to make a homogeneous solution. Water was evaporated at 60 °C in a Petri dish. The dry powder was heated at 500 °C in synthetic air for 1 h with ramp of 2 °C $min^{-1}$ and cooled down naturally to room temperature. The solid powder was collected and designated as **B-$Co_2Mn$**.

**Table S1. Characterization of the catalysts**

| Catalysts | Initial atomic ratio of Co/Mn during synthesis | Co/Mn atomic ratio in bulk by ICP-AES analyses |
|---|---|---|
| **$Co_2Mn$** | 2 | 1.74 |
| **CoMn** | 1 | 0.98 |
| **$CoMn_2$** | 0.5 | 0.48 |

**Electrode preparation**

30 mg of catalyst powder was taken in a glass vial and iodine (10 mg) solution in acetone (6 mL) was added to it. The mixture was placed in an ultrasonic bath and sonicated for 30 minutes at room temperature to get a well dispersed catalyst system. The electrodes were prepared by electrophoretic deposition with a potential difference of 10 V on 1x1 $cm^2$ area of Ni foam (Racemat BV, both anode and cathode) for 5 minutes.[S2] Electrophoretic deposition involves migration of the charged particles from the suspension to the electrode surface under the influence of an applied electric field. The particle packing on the surface of the electrode largely depends on the electric field strength. Iodine in acetone medium forms charged species, which are adsorbed on the surface of the catalyst and promote the migration of the particles.

**Electrochemical measurements**

Cyclic voltammetry (CV) and chronoamperometric studies were carried out in 1 M aqueous KOH solution by using single-compartment three-electrode electrochemical cell (catalyst deposited on Ni foam as working electrode, Pt wire as a counter electrode and $Hg/Hg_2SO_4$ as a reference electrode) by using potentiostat (SP-200, BioLogic Science Instruments) run by EC-Lab v10.20 software package Electrochemical impedance spectroscopic (EIS) measurements were performed with frequency from 0.1 to 100,000 Hz and amplitude of 5 mV at constant potential of 1.41 V vs RHE and iR correction has been performed from the $R_u$ values. All the potential values were converted to the reversible hydrogen electrode (RHE) in 1 M aqueous KOH solution (pH 14):

$E(RHE) = E(Hg/Hg_2SO_4) + 0.64 + 0.059pH$

**Figures**

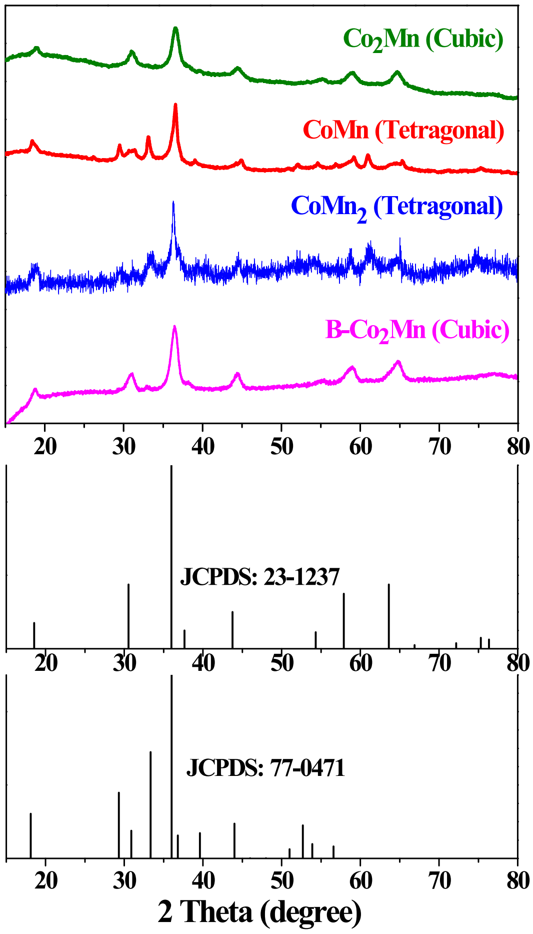

**Fig. S1**. PXRD patterns of spinel cobalt manganese oxides representing cubic phase for **$Co_2Mn$** and **B-$Co_2Mn$** (JCPDS 23-1237, space group *Fd*3*m*, Nr. 227) and tetragonal phases (JCPDS 77-471, space group *I*41/*amd*, Nr. 141) for **CoMn** and **$CoMn_2$**.

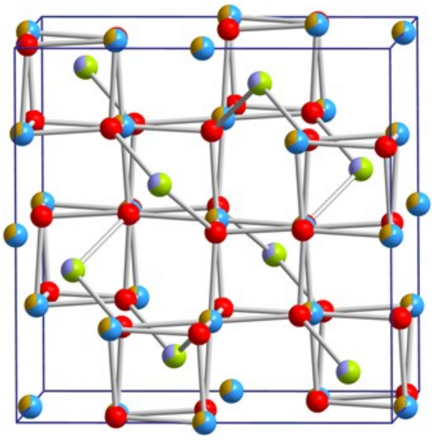

**Fig. S2.** General representation of the crystal structures of **$Co_2Mn$, CoMn** and **$CoMn_2$** of a spinel oxide system. Both the cubic and tetragonal phases of cobalt manganese oxides belong to mixed-valent spinel structures where mixed occupancy of Co and Mn ions over tetrahedral (*Td,* mixed blue-orange balls) and octahedral (*Oh,* mixed violet-green balls) sites could be established. Red balls represent oxygen atoms.

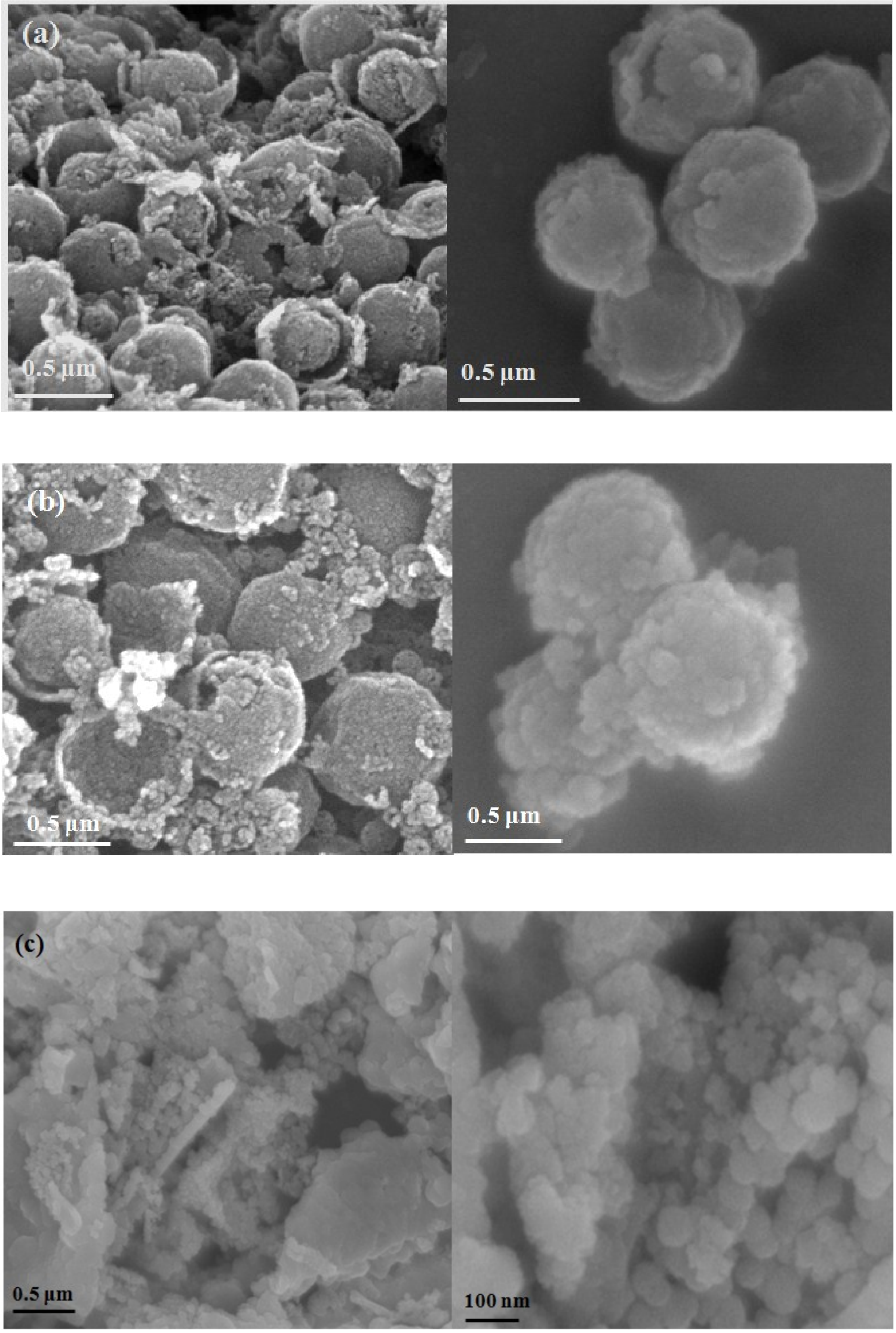

**Fig. S3**. SEM images showing spherical morphology of the cobalt manganese oxide particles with hollow multi layers inside particles for (a) **CoMn** and (b) **$\mathbf{CoMn_2}$**. (c) SEM image of bulk cobalt manganese oxide **$\mathbf{B\text{-}Co_2Mn}$.**

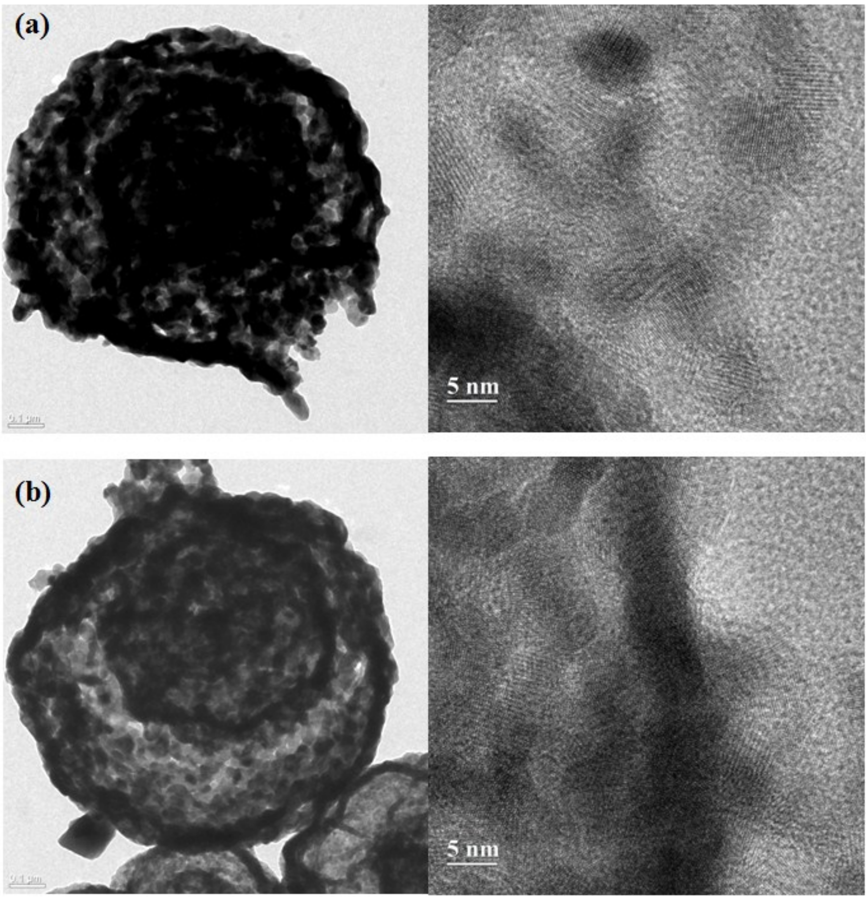

**Fig. S4**. TEM and corresponding HRTEM images of (a) **CoMn** and **(b) CoMn$_2$**. TEM images clearly show the multi layered hollow spherical morphology of the cobalt manganese oxide particles.

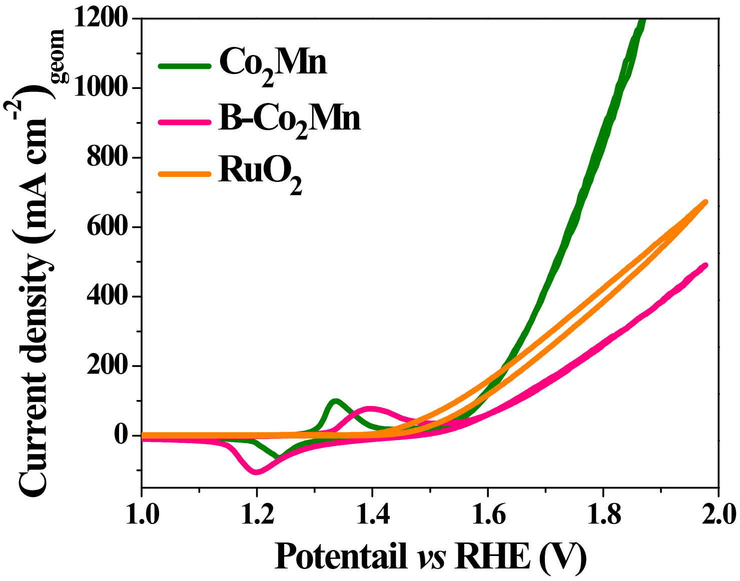

**Fig. S5**. Comparison of the water oxidation catalytic activities of the multi shelled cobalt manganese oxides with noble metal catalyst RuO$_2$ and bulk Co$_2$MnO$_4$ (**B-Co$_2$Mn**) in 1 M aqueous KOH solution.

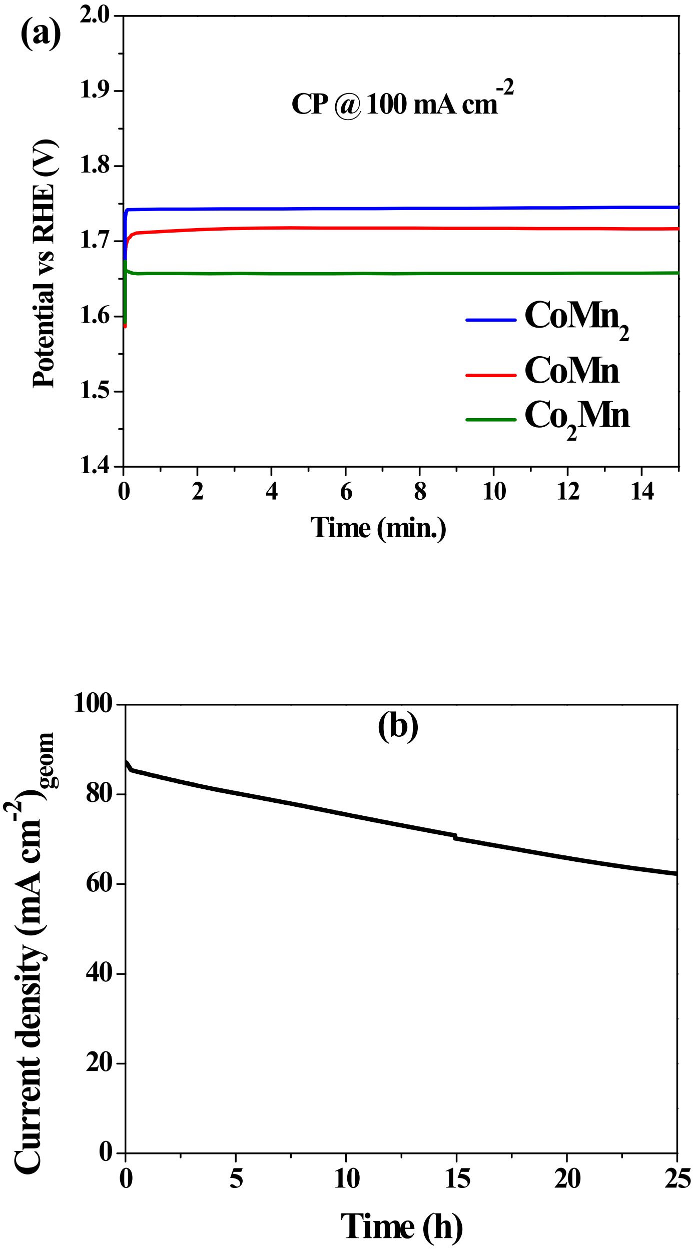

**Fig. S6**. (a) Chronopotentiometric measurements with the multi shelled hollow microspheres in 1 M aqueous KOH solution at current density 100 mA cm$^{-2}$ to find out the real overpotential under steady state conditions to avoid capacitance current due to polarization (without iR correction) and (b) chronoamperometric studies of multi shelled hollow **$Co_2Mn$** in 1 M aqueous KOH solution at potential 1.61V showing ~ 25% drop compared to initial current density after 24 h electrochemical measurements (without iR correction).

**Table S2**. Comparison of the catalytic activities of multi shelled cobalt manganese oxides hollow spheres with literature reported transition metal oxide catalysts deposited on Ni foam.

| Catalyst | Aqueous electrolyte solution | Current density (mA $cm^{-2}$) | Overpotential (mV) | Reference |
|---|---|---|---|---|
| $Co_3O_4$ @Ni foam | 1 M KOH | 10 | 328 (from polarization curve) | S3 |
| FeOOH@Ni foam | 1 M NaOH | 10 | 290 (from polarization curve) | S4 |
| $Ni_3S_2$@Ni foam | 0.1 M KOH | 10 | 187 (from polarization curve) | S5 |
| $Ni_3N$@Ni foam | 1 M KOH | 20 | 390 (from polarization curve) | S6 |
| $Mn_3O_4$@Ni foam | 1 M KOH | 10 | 270 (from polarization curve) | S7 |
| NiO@Ni foam | 1 M KOH | 10 | 345 (from polarization curve) | S8 |
| $NiSe_2$-graphene@Ni foam | 0.1 M KOH | 20 | 307 from polarization curve | S9 |
| FeOOH/$CeO_2$@Ni foam | 1 M NaOH | 20 | 240 (from polarization curve) | S10 |
| Porous carbon- Ni@Ni foam | 0.1 M KOH | 10 | 520 (from polarization curve) | S11 |
| $MoS_2$@Ni foam | 1 M NaOH | 20 | 310 (from polarization curve) | S12 |
| Ni-Fe-OH@$Ni_3S_2$@Ni foam | 1 M KOH | 10 | 165 (from polarization curve) | S13 |
| CoO-graphene@ Ni foam | 0.1 M KOH | 10 | 330 from polarization curve | S14 |
| $Ni_3Se_2$@Ni foam | 0.3 M KOH | 10 | 290 from polarization curve | S15 |
| $Co_2MnO_4$@Ni foam | 1 M KOH | **100** | **360** from polarization curve | This work |
| $Co_{1.5}Mn_{1.5}O_4$@Ni foam | 1 M KOH | **100** | **390** (from polarization curve) | This work |
| $CoMn_2O_4$@Ni foam | 1 M KOH | **100** | **430** (from polarization curve) | This work |
| $Co_2MnO_4$@Ni foam | 1 M KOH | **100** | **430** (under steady state) | This work |
| $Co_{1.5}Mn_{1.5}O_4$@Ni foam | 1 M KOH | **100** | **470** (under steady state) | This work |
| $CoMn_2O_4$@Ni foam | 1 M KOH | **100** | **510** (under steady state) | This work |

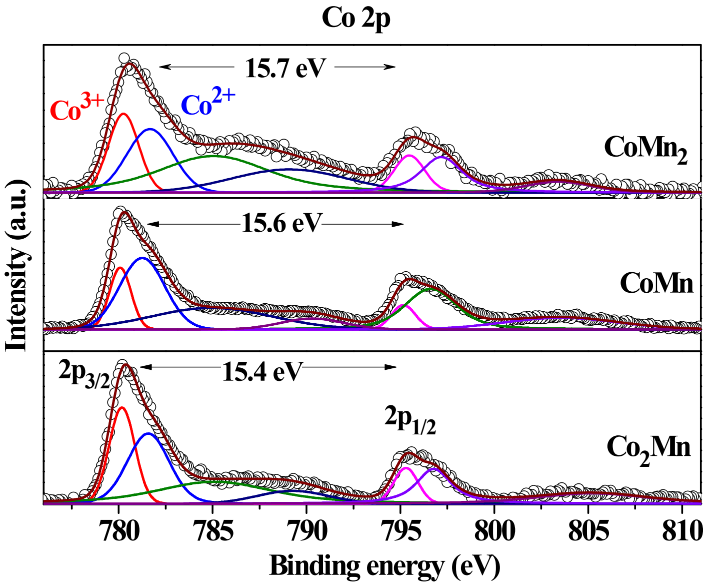

**Fig. S7**. Co 2p edge XPS studies of the fresh cobalt manganese oxides showed that Co is in mixed valence (+2 and +3) states and occupied both tetrahedral and octahedral sites.

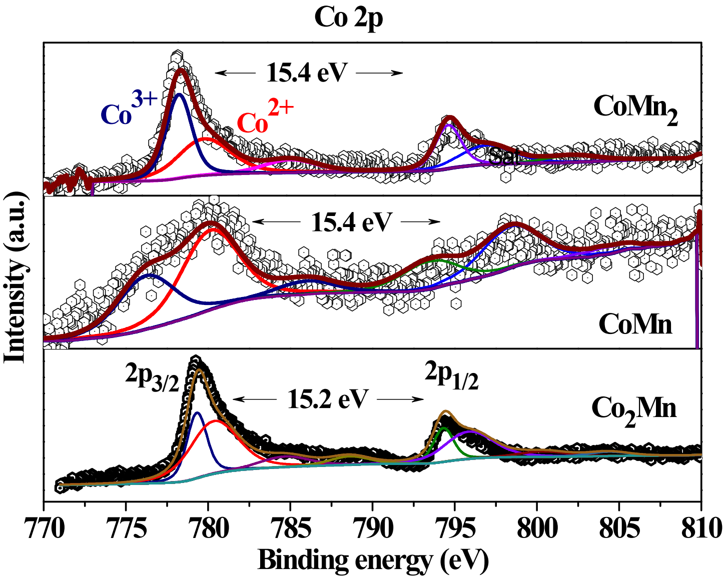

**Fig. S8**. Co 2p edge XPS studies of the cobalt manganese oxides after chronoamperometric measurements showed that partial oxidation of $Co^{2+}$ to $Co^{3+}$ during alkaline water oxidation.

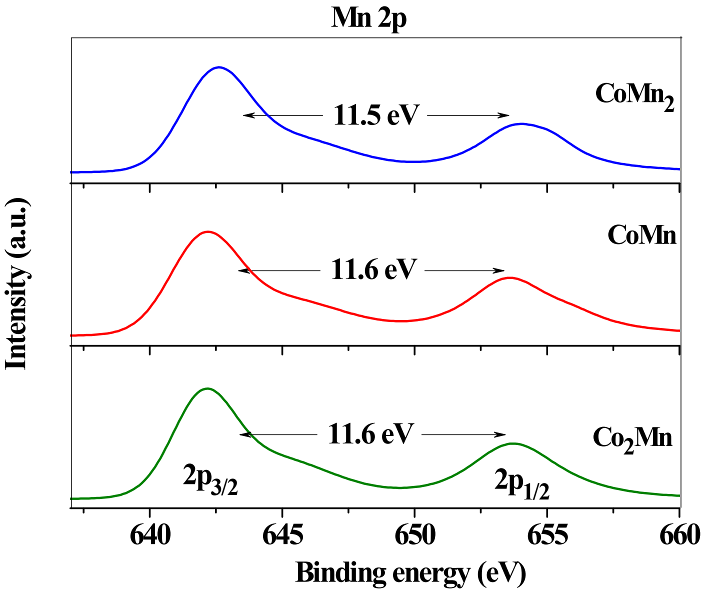

**Fig. S9**. Mn 2p edge XPS studies of the fresh cobalt manganese oxides showed that Mn is in mixed valence (+2 and +3) states and occupied both tetrahedral and octahedral sites.

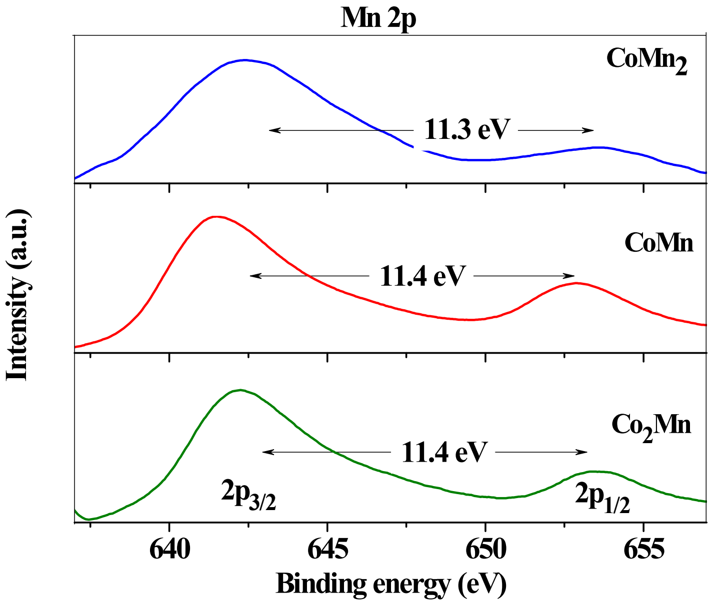

**Fig. S10**. Mn 2p edge XPS studies of the cobalt manganese oxides after chronoamperometric measurements showed that partial oxidation of $Mn^{2+}$ to $Mn^{3+}$ during alkaline water oxidation.

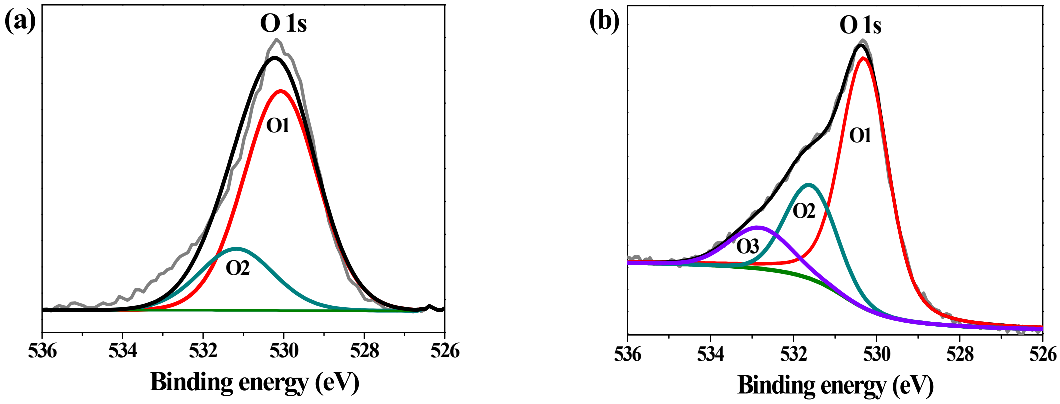

**Fig. S11**. O 1s edge XPS studies of cobalt manganese oxide **Co$_2$Mn** (a) fresh and (b) after chronoamperometric measurements showed hydroxylation and hydration of the catalyst surface during alkaline water oxidation. The peak O1 is assigned to the metal-oxygen bond, peak O2 is for –OH species and the peak O3 is from adsorbed water molecules at the surface.

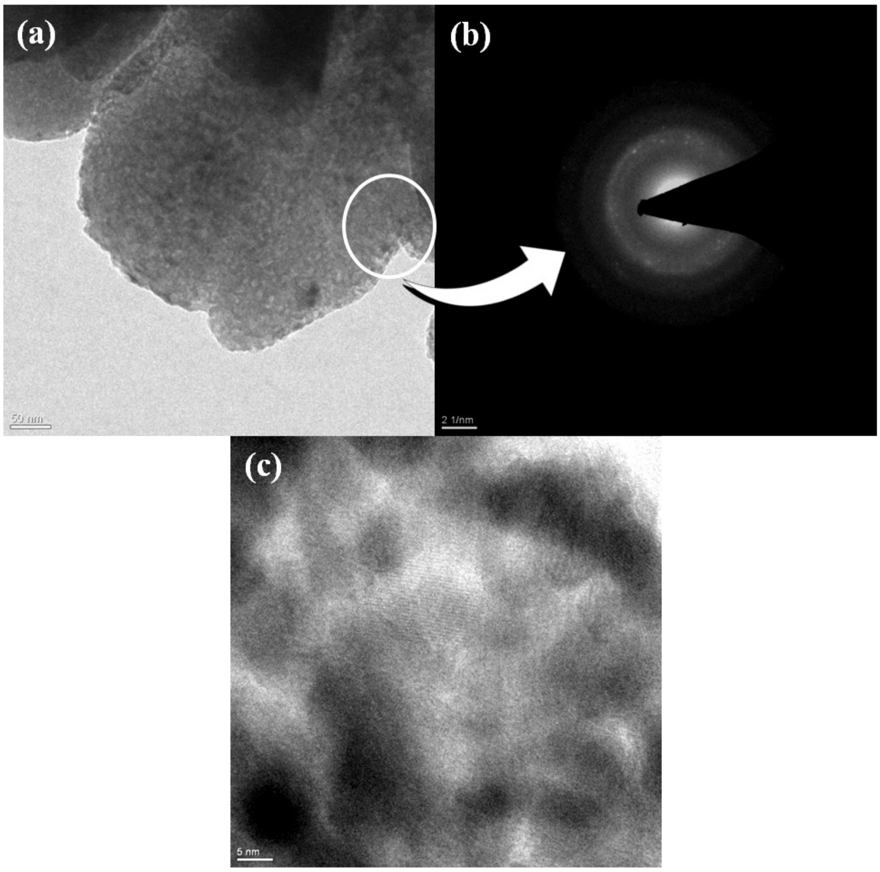

**Fig. S12**. (a) TEM image of the **Co$_2$Mn** after chronoamperometric measurements of 24 h showing amorphous phase formation, (b) selected area diffraction pattern and (c) HRTEM to show mostly the amorphous nature.

## References

S1. Q. Wang, H. Li, L. Chen and X. Huang, *Solid State Ionics* 2002, **152**, 43-50.

S2. J. Pfrommer, M. Lublow, A. Azarpira, C. Göbel, M. Lücke, A. Steigert, M. Pogrzeba, P. W. Menezes, A. Fischer, T. Schedel-Niedrig and M. Driess, *Angew. Chem. Int. Ed.* 2014, **53**, 5183-5187.

S3. A. J. Esswein, M. J. McMurdo, P. N. Ross, A. T. Bell and T. D. Tilley, *J. Phys. Chem. C* 2009, **113**, 15068-15072.

S4. B. Lu, C. Wang, S. Chen,Y. Jinling, G. Wang and D. Cao, *J. Solid State Electrochem* 2013, **17**, 2277-2282.

S5. W. Zhou, X. Wu, X. Cao, X. Huang, C. Tan, J. Tian, H. Liu, J. Wang and H. Zhang, *Energy Environ. Sci.* 2013, **6**, 2921-2924.

S6. M. Shalom, D. Ressnig, X. Yang, G. Clavel, T. P. Fellinger and M. Antonietti, *J. Mater. Chem. A*, 2015, **3**, 8171-8177.

S7. M. Q. Yu, Y. H. Li, S. Yang, P. F. Liu, L. F. Pan, L. Zhang and H. G. Yang, *J. Mater. Chem. A*, 2015, **3**, 14101-14104.

S8. J. Liang, Y. Wang, C.Wanga and S. Lu, *J. Mater. Chem. A*, 2016, **4**, 9797-9806.

S9. J. Yu, Q. Li, C. Xu, N. Chen, Y. Li, H. Liu, L. Zhen, V. P. Dravida and J. Wu, *J. Mater. Chem. A*, 2017, **5**, 3981-3986.

S10. J. Feng, S. Ye, Han Xu, Y. Tong and G. Li, *Adv. Mater.* 2016, **28**, 4698-4703.

S11. J. Wang, H. Zhong, Y. Qin and X. Zhang, *Angew. Chem. Int. Ed.* 2013, **52**, 5248 -5253.

S12. K. Yan and Y. Lu*,* *Small* 2016, **12**, 2975-2981.

S13. X. Zou, Y. Liu, G. Li, Y. Wu, D. Liu, W. Li, H. Li, D. Wang, Y. Zhang and X. Zou, *Adv. Mater.* 2017, 1700404.

S14. W. Yuan, M. Zhao, J. Yuan, C. M. Li, *J. Power Sources* 2016, **319**, 159-167.

S15. A. T. Swesi, J. Masud and M. Nath, *Energy Environ. Sci.* 2016, **9**, 1771-1782.